Efficient CO_2 capture by tertiary amine-functionalized ionic liquids through Li^+-stabilized zwitterionic adduct formation

Zhen-Zhen Yang and Liang-Nian He[*]

Full Research Paper

Abstract

Highly efficient CO_2 absorption was realized through formation of zwitterionic adducts, combining synthetic strategies to ionic liquids (ILs) and coordination. The essence of our strategy is to make use of multidentate cation coordination between Li^+ and an organic base. Also PEG-functionalized organic bases were employed to enhance the CO_2-philicity. The ILs were reacted with CO_2 to form the zwitterionic adduct. Coordination effects between various lithium salts and neutral ligands, as well as the CO_2 capacity of the chelated ILs obtained were investigated. For example, the CO_2 capacity of $PEG_{150}MeBu_2N$ increased steadily from 0.10 to 0.66 (mol CO_2 absorbed per mol of base) through the formation of zwitterionic adducts being stabilized by Li^+.

Introduction

Carbon capture and sequestration (CCS) from flue gas formed by combustion of fossil fuel is a critical part of efforts directed towards the stabilization of atmospheric greenhouse gas levels [1]. In recent years, there has been intense research worldwide aimed at the development of various processes and technologies for efficient CO_2 capture. These efforts include the development of liquid and solid absorbents and membranes [2-7].

Ionic liquids (ILs), which have attractive properties such as negligible vapor pressure, a wide liquid temperature ranges, good thermal stability, high ionic conductivity, and versatile solvation properties [8-11], can be designed for task-specific applications through the smart choice of the respective cations and/or anions. Application fields include green solvents for synthesis [9,12-15], efficient catalysts in organic synthesis [2,16,17], media for advanced separation [18,19], novel electrolytes for energy applications [20,21], and efficient absorbents for gas separation [2,22-24]. In particular, amino-functionalized IL [APBIm][BF_4] (1-aminopropyl-3-butylimidazolium tetrafluoroborate) and ILs being composed of amino acid (AA) anions and phosphonium or ammonium cations were developed for efficient CO_2 chemisorption [23,25-30]. Binary absorbents derived from superbases together with various non-volatile

weak proton donors such as hydroxy-functionalized ILs, imidazolium ILs, fluorinated alcohol, imidazole and phenol, were also found to be efficient liquid absorbents allowing for reversible CO_2 chemisorption [31-35]. In general, two absorbent molecules are involved to react with one CO_2 molecule generating ammonium carbamate (Scheme 1a) or ammonium alkyl formate (Scheme 1b). Hence, increasing the 1:2 (CO_2:absorbent molecule) stoichiometry for the CO_2 capacity to 1:1 is an essential prerequisite for a breakthrough in absorption techniques [23]. In this respect, task-specifically designed absorbents have been successfully synthesized from AAs and applied for 1:1 CO_2 capture through a carbamic acid formation pathway (Scheme 1a, step 1). Notably, equimolar CO_2 absorption was obtained using task-specific ionic liquids (TSILs) with the phosphonium cation containing long alkyl chains and anions derived from AAs (prolinate and methioninate) [36], or AA salts with bulky N-substituents in polyethylene glycol (PEG) solution [37]. However, procedures for the preparation of ILs usually include complicated purification procedures or the use of volatile organic solvents (e.g., toluene, acetonitrile). Recently, Wang et al. developed novel alkanolamine-based ILs through multi-dentate cation coordination between alkanolamine and Li^+ for reversible CO_2 capture, by simple mixing of equimolar amounts of alkanolamines with $LiNTf_2$ [38]. The strong complexation of alkali metal cations by crown ethers could be used to achieve equimolar CO_2 absorption in systems containing crown ethers and easily available alkali metal salts of amino acids, resulting in the respective carbamates (onium salts) [39].

As previously reported, strong amidine and guanidine bases such as 1,5,7-triazabicyclo[4.4.0]dec-5-ene (TBD) can form the base-CO_2 zwitterionic adduct in a 1:1 manner under strictly anhydrous conditions (Scheme 1c) [40,41]. Herein, we present such a method combining the formation of ILs and coordination to achieve equimolar CO_2 capture through zwitterionic adduct formation. The essence of our strategy is to make use of the multisite coordination interaction between Li^+ and organic bases or PEG-functionalized organic bases. The readily prepared ILs were reacted then with CO_2 to form intramolecular zwitterionic adducts.

Results and Discussion

Taking $PEG_{150}MeTMG$ as a neutral ligand (Table 1), coordination effects of various lithium salts were investigated (Table S1, Supporting Information File 1). Only $LiSO_3CF_3$ and $LiNTf_2$ formed complexes with $PEG_{150}MeTMG$ through multisite coordination. Subsequently, different neutral ligands with alkyl chains or PEG chain were selected to evaluate the effect of chelating with $LiNTf_2$ on the physicochemical properties of the resulting ILs as well as the CO_2 capacities (Table 1).

Typical optimized structures of cations derived from chelation between neutral ligands and Li^+ are shown in Figure 1. The geometry optimizations were carried out by performing DFT calculations. Four O atoms in $PEG_{150}Me$ chelate with Li^+ in a quasi-crown ether manner. For neutral ligands with PEG chain ($PEG_{150}MeIm$, $PEG_{150}MeNH_2$, $PEG_{150}MeTMG$ and $PEG_{150}MeBu_2N$), all the O and N atoms coordinate with Li^+ in a quasi-aza-crown ether fashion. OctIm, OctTMG, TMG, DBU and DBN generate complexes whereby Li^+ is bound only to N atoms. In contrast, the coordination ability of the N atom in $OctBu_2N$ is not strong enough to form a homogeneous chelated IL with $LiNTf_2$.

Calculation of the energy of the gas phase reaction between neutral ligands and Li^+ gave a value for the enthalpy change in the range of −41.59 to −106.56 kcal mol^{-1} (Table 1, entries 1–11), indicating that the formation of chelated ILs is feasible.

In addition, PEG-functionalization of the organic base enhanced the complexation ability. For example, ΔH_f decreased from −56.49 kal mol^{-1} (OctIm) to −91.17 kcal mol^{-1} ($PEG_{150}MeIm$) for imidazole (Table 1, entry 2 vs 3), from −47.79 kcal mol^{-1} (OctTMG) to −106.56 kcal mol^{-1} ($PEG_{150}MeTMG$) for guanidine (Table 1, entry 6 vs 7), and from no complexation ($OctBu_2N$) to −96.26 kal mol^{-1} ($PEG_{150}MeBu_2N$) for tertiary amine (Table 1, entry 8 vs 9).
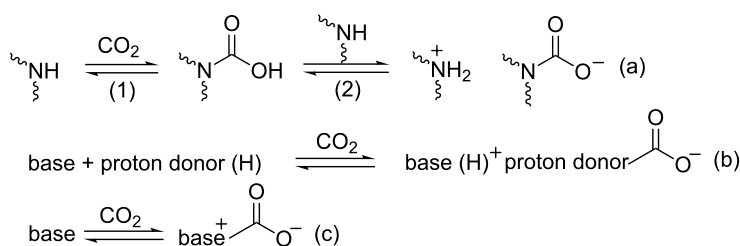
Scheme 1: Reactions of CO_2 with amino-group containing absorbents (a), base/proton donor binary system (b) or strong organic base (c).

Table 1: Stability (ΔH_f) of the cations derived from coordination of Li^+ in $LiNTf_2$ with various neutral ligands and CO_2 capacity of the derived ionic liquids[a].

PEG$_{150}$Me   PEG$_{150}$MeNH$_2$ PEG$_{150}$MeIm   OctIm

TMG   OctTMG   PEG$_{150}$MeTMG

OctBu$_2$N   PEG$_{150}$MeBu$_2$N   DBN   DBU

Entry	Ionic liquid	ΔH_f/kcal mol^{-1} [b]	CO_2 capacity[c]
1	[PEG$_{150}$MeLi][NTf$_2$]	−100.94	0.09 (0.9%)
2	[OctImLi][NTf$_2$]	−56.49	0.11 (1.0%)
3	[PEG$_{150}$MeImLi][NTf$_2$]	−91.17	0.16 (1.4%)
4	[PEG$_{150}$MeNH$_2$Li][NTf$_2$]	−89.39	0.45 (4.4%)
5	[TMGLi][NTf$_2$]	−41.59	0.65 (7.1%)
6	[OctTMGLi][NTf$_2$]	−47.79	0.80 (6.8%)
7	[PEG$_{150}$MeTMGLi][NTf$_2$]	−106.56	0.89 (7.1%)
8	OctBu$_2$N/LiNTf$_2$	–	–
9	PEG$_{150}$MeBu$_2$N	–	0.10 (1.6%)
10	[PEG$_{150}$MeBu$_2$NLi][NTf$_2$]	−96.26	0.66 (5.2%)
11	[PEG$_{150}$MeBu$_2$NLi][SO$_3$CF$_3$]	−96.26	0.61 (6.2%)
12	[DBULi][NTf$_2$]	−60.22	0.50 (5.0%)
13	[DBNLi][NTf$_2$]	−60.50	0.75 (8.0%)

[a]Ionic liquids were prepared by mixing of a neutral ligand with $LiNTf_2$ in 1:1 molar ratio. CO_2 absorption was carried out at 25 °C and absorption equilibrium was reached within 20 min. [b]Energy of the gas phase reaction between the neutral ligand and Li^+, was calculated with DFT, using the B3PW91 functional with the 6-311++G (d,p) basis set as implemented in the Gaussian 09 program package. [c]Mol of CO_2 captured per mol of ionic liquid. Results in bracket were grams of CO_2 absorbed per gram of absorbent.

The structures of the chelated ILs were confirmed by thermogravimetric analysis (TGA), NMR (see Supporting Information File 1, Figure S2), in situ FTIR under CO_2 pressure and mass spectrometry. The thermal stability of the chelated ILs was strongly increased compared to the corresponding neutral ligands. The decomposition temperature increased by 90 °C and 60 °C for PEG$_{150}$MeTMG and PEG$_{150}$MeBu$_2$N, respectively, after coordination with $LiNTf_2$ (Figure 2a).

In the ^{1}H NMR spectrum, the proton signals of the four methyl groups in guanidine of PEG$_{150}$MeTMG shifted from 2.63–2.72 ppm to 2.96 ppm after reacting with equimolar amounts of $LiNTf_2$ (Figure 2b). The corresponding anion $CF_3SO_3^-$, the twelve protons moving only from 2.63–2.72 ppm to 2.71–2.75 ppm, indicate that there is only little influence of the anion on the nature of the coordinative bond. In the case of tertiary amines (e.g., PEG$_{150}$MeBu$_2$N), all the protons shifted downfield after forming the chelated IL with $LiNTf_2$. Changing

the anion to $CF_3SO_3^-$ had negligible influence on the coordination ability. All the neutral ligands shown in Table 1 gave a downfield shift in the ^{1}H NMR spectrum after chelating with Li^+, in accordance with the electron density decreasing through coordination. Furthermore, the formation of chelated ILs was also verified by ESI-MS (m/z = 268.27 for [PEG$_{150}$MeTMGLi]$^+$ and m/z = 282.32 for [PEG$_{150}$MeBu$_2$NLi]$^+$) (Figure S3, see Supporting Information File 1). In the in situ FTIR spectrum, the C=N absorption band of the neutral ligand PEG$_{150}$MeTMG was shifted from 1616 cm^{-1} to 1592 cm^{-1} after reacting with equimolar amounts of $LiNTf_2$ as depicted in Figure 3a.

The effect of various chelated ILs on CO_2 absorption was subsequently examined using $LiNTf_2$ as coordinating reagent. The CO_2 absorption capacity, defined as mol of CO_2 captured per mol of IL, was estimated from the weight increase of the reaction mixture. As shown in Table 1, ILs of weak basicity,
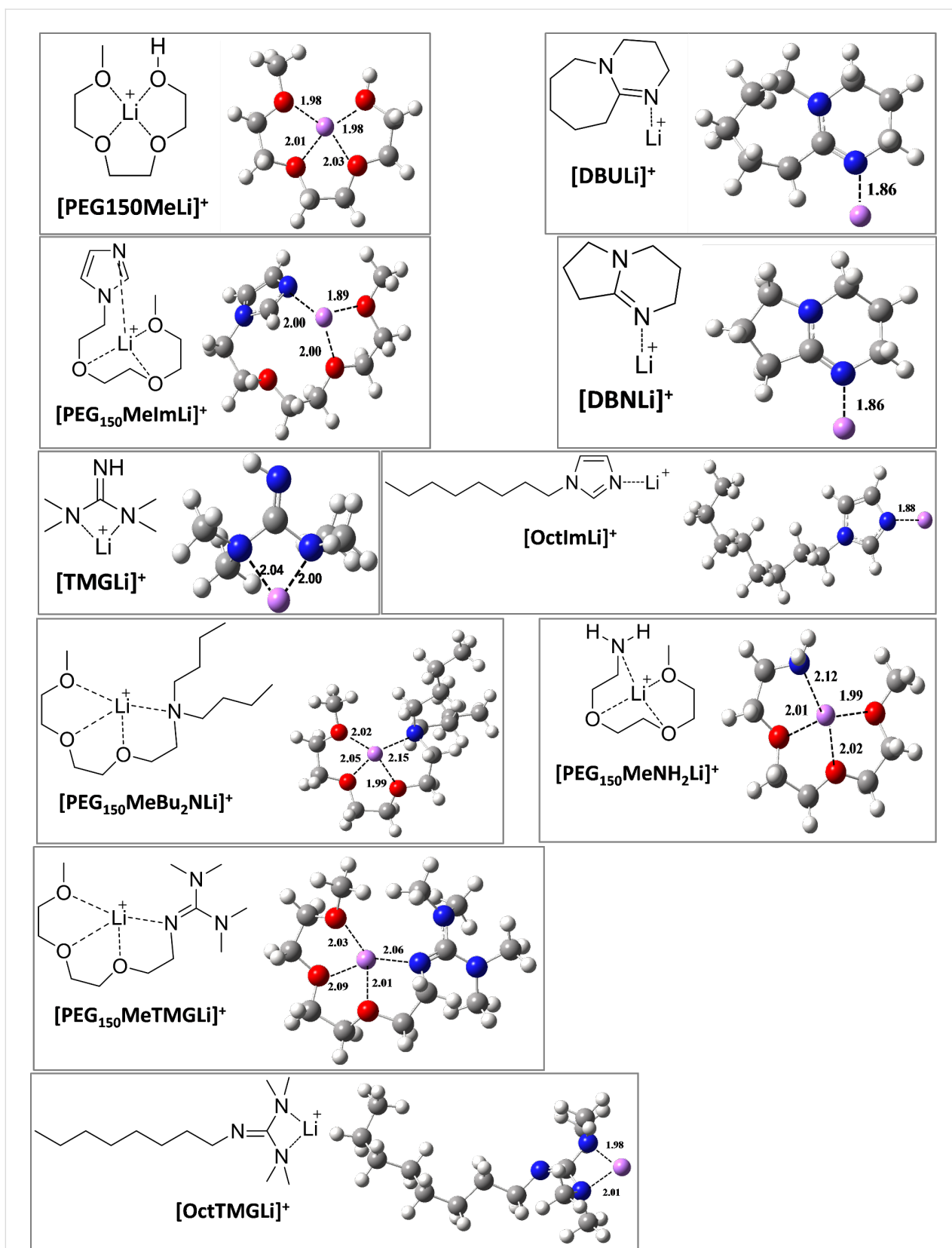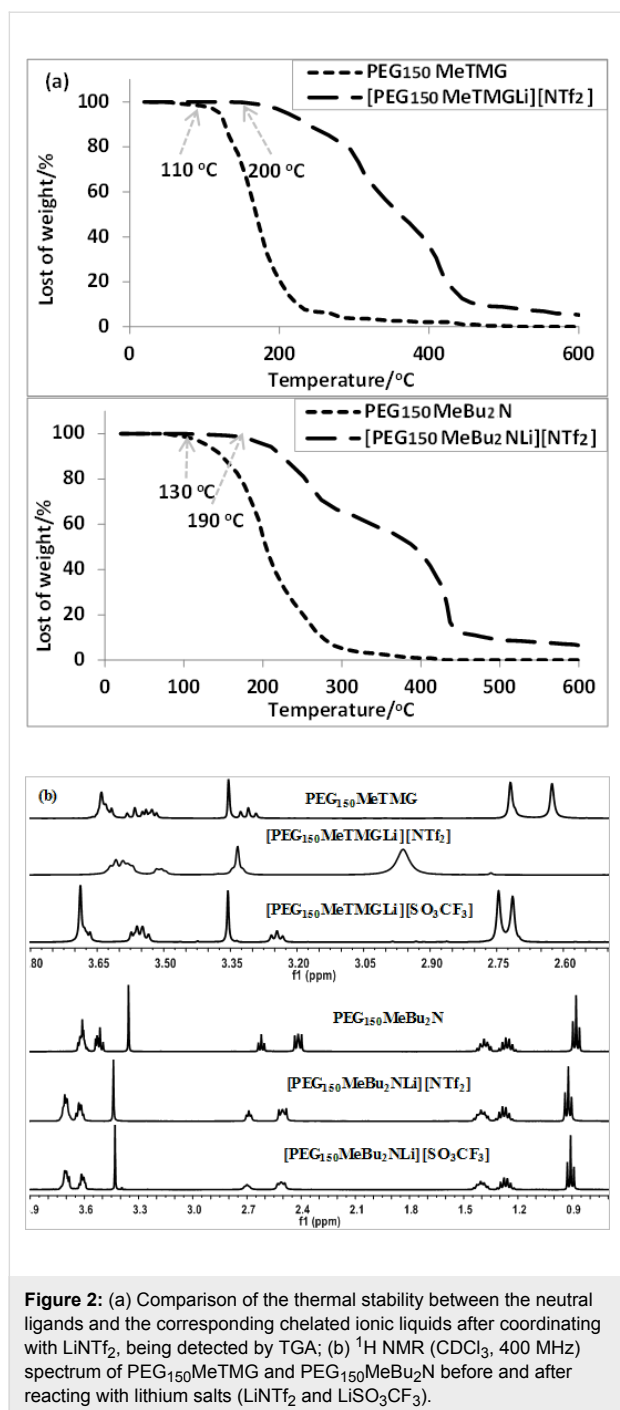
Figure 1: Typical optimized structures of complex cations derived from chelation between Li$^+$ and neutral ligands. H: white, C: grey, O: red, N: blue, Li: purple. Bond lengths are in Å.
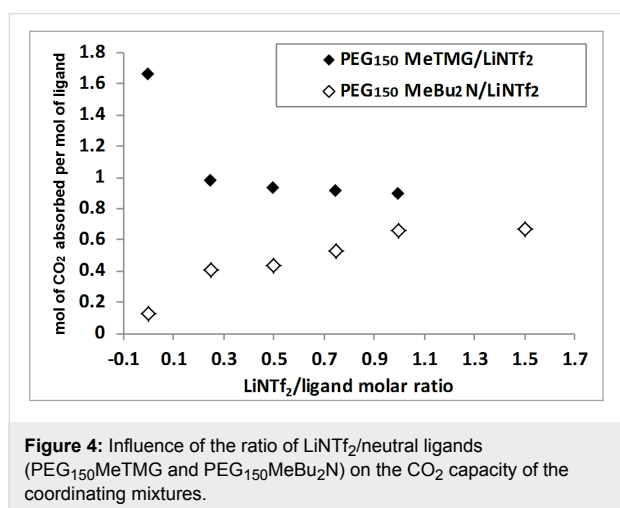
Figure 2: (a) Comparison of the thermal stability between the neutral ligands and the corresponding chelated ionic liquids after coordinating with LiNTf$_2$, being detected by TGA; (b) ^{1}H NMR (CDCl$_3$, 400 MHz) spectrum of PEG$_{150}$MeTMG and PEG$_{150}$MeBu$_2$N before and after reacting with lithium salts (LiNTf$_2$ and LiSO$_3$CF$_3$).

Figure 3: In situ FTIR spectra of neutral ligands and the corresponding chelated ionic liquids after reaction with LiNTf$_2$, as well as the reaction mixture after CO$_2$ absorption in the absence or presence of water.

such as [PEG$_{150}$MeLi][NTf$_2$], [OctImLi][NTf$_2$] and [PEG$_{150}$MeImLi][NTf$_2$] showed a poor CO$_2$ sorption capacity, implying that only physical interactions with CO$_2$ were present (Table 1, entries 1–3). The primary amine-functionalized IL [PEG$_{150}$MeNH$_2$Li][NTf$_2$] gave rise to CO$_2$ uptake approaching 1:2 stoichiometry (Table 1, entry 4) as expected from the proposed mechanism for the formation of ammonium carbamate as shown in Scheme 1a [38]. Notably, the CO$_2$ capacity of guanidine-functionalized ILs increased in the order of
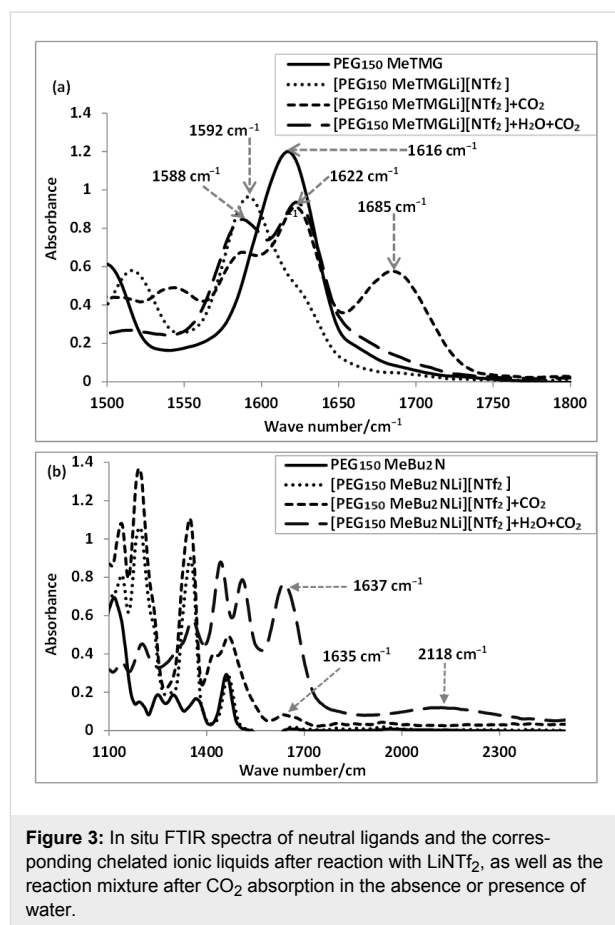
[TMGLi][NTf$_2$] (0.65) < [OctTMGLi][NTf$_2$] (0.80) < [PEG$_{150}$MeTMGLi][NTf$_2$] (0.89 mol CO$_2$ absorbed per mol of base) (Table 1, entries 5–7), indicating that the CO$_2$-philic nature of the PEG chain facilitates CO$_2$ sorption. Generally, anhydrous tertiary amines absorb CO$_2$ only under high CO$_2$ pressures to form instable zwitterionic alkylcarbonate salts (Table 1, entry 9) [42]. [PEG$_{150}$MeBu$_2$NLi][NTf$_2$] and [PEG$_{150}$MeBu$_2$NLi][SO$_3$CF$_3$] were able to rapidly reach 0.66 and 0.61 CO$_2$ capacity, respectively. Thus, tertiary amino-functionalized ILs with multidentate cation coordination have a much better performance probably due to the formation of a zwitterionic adduct being stabilized by Li$^+$ (Table 1, entries 10 and 11). Indeed, the CO$_2$ absorption capacity of [PEG$_{150}$MeBu$_2$NLi][NTf$_2$] increased steadily from 0.10 to 0.66 mol CO$_2$ absorbed per mol of base when the molar ratio of LiNTf$_2$/PEG$_{150}$MeBu$_2$N was varied from 0 to 1. When the molar ratio was increased to 1.5, no further promotion of the CO$_2$ capacity was observed (Figure 4). In contrast, when PEG$_{150}$MeTMG was employed as the neutral ligand, the CO$_2$ capacity decreased from 1.66 to 0.89 mol CO$_2$ absorbed per mol of base as the molar ratio of LiNTf$_2$/PEG$_{150}$MeTMG was increased from 0 to 1, probably due to decreased basicity of guanidine after coordinating with Li$^+$. At last, ILs

[DBULi][NTf$_2$] (0.50) and [DBNLi][NTf2] (0.75 mol CO$_2$ absorbed per mol of base) had a CO$_2$ capacity below 1:1 stoichiometry expected from the proposed mechanism (Scheme 1c), owing to highly increased viscosity after CO$_2$ absorption (Table 1, entries 12 and 13). Compared on a weight basis, a CO$_2$ capacity of 5.0 wt % to 8.0 wt % was obtained with ILs from neutral ligands/LiNTf$_2$ (Table 1, entries 5–7 and 10–13). This is much higher than for the conventional IL 1-hexyl-3-methylimidazolium hexafluorophosphate (0.0881 wt %) [43], and comparable to amino-functionalized imidazolium-based IL (7.4 wt %) [23] and ILs derived from amino acids [24]. Hence, our IL system has the potential to be utilized for industrialized CO$_2$ absorption processes.

Figure 4: Influence of the ratio of LiNTf$_2$/neutral ligands (PEG$_{150}$MeTMG and PEG$_{150}$MeBu$_2$N) on the CO$_2$ capacity of the coordinating mixtures.

The in situ FTIR spectrum of [PEG$_{150}$MeTMGLi][NTf$_2$] and [PEG$_{150}$MeBu$_2$NLi][NTf$_2$] before and after reaction with CO$_2$ are shown in Figure 3. For [PEG$_{150}$MeTMGLi][NTf$_2$] as absorbent, the C=N stretching band at 1592 cm^{-1} shifted to 1622 cm^{-1} after reaction with CO$_2$. A characteristic peak centered at 1685 cm^{-1} is assigned to the stretching vibration of the carbonyl group in the zwitterionic alkyl carbamate, which is quite different from that in HCO$_3^-$ (1588 cm^{-1}). For the reaction of [PEG$_{150}$MeBu$_2$NLi][NTf$_2$] with CO$_2$, a new band at 1635 cm^{-1} was assigned to the stretching vibration of the C=O bond in the zwitterionic product. In addition, a distinct broad band at around 2118 cm^{-1} corresponding to the ammonium cation was observed in the presence of water.

To gain deeper insight into the reaction mechanism of CO$_2$ absorption with chelated ILs, DFT calculations were carried out. We performed geometry and energy optimizations for the free [BaseLi]$^+$ cation, free CO$_2$ and the [BaseLi]$^+$ + CO$_2$ complex. As shown in Figure 5, the chelated ILs react with CO$_2$ through nucleophilic attack by the N atom, to form the zwitterionic adducts, which are stabilized through coordination

with Li$^+$. In addition, formation of the zwitterionic alkyl carbamate is calculated to be associated with an enthalpy changes of −102.36 kcal mol^{-1} and −89.50 kcal mol^{-1} for [PEG$_{150}$MeTMGLi]$^+$/CO$_2$ and [PEG$_{150}$MeBu$_2$NLi]$^+$/CO$_2$, respectively, indicating that the absorption process is thermodynamically favourable.

Conclusion

In summary, efficient CO$_2$ capture was achieved through formation of zwitterionic adducts with readily synthesized chelated ILs. Multisite coordination interaction between the Li$^+$ cation and organic bases or PEG-functionalized organic bases is thought to be responsible for forming the amidine, guanidine or tertiary amine-functionalized ILs, after reaction with CO$_2$ to form zwitterionic adducts in a 1:1 manner. Coordination effects between various lithium salts and neutral ligands, and the CO$_2$ capacity of the obtained chelated ILs were investigated. Indeed, the thermal stability and the CO$_2$ capacity of the neutral ligands (e.g., PEG$_{150}$MeBu$_2$N) was highly increased after coordination with lithium salts to form chelated ILs (e.g., [PEG$_{150}$MeBu$_2$NLi][NTf$_2$]).
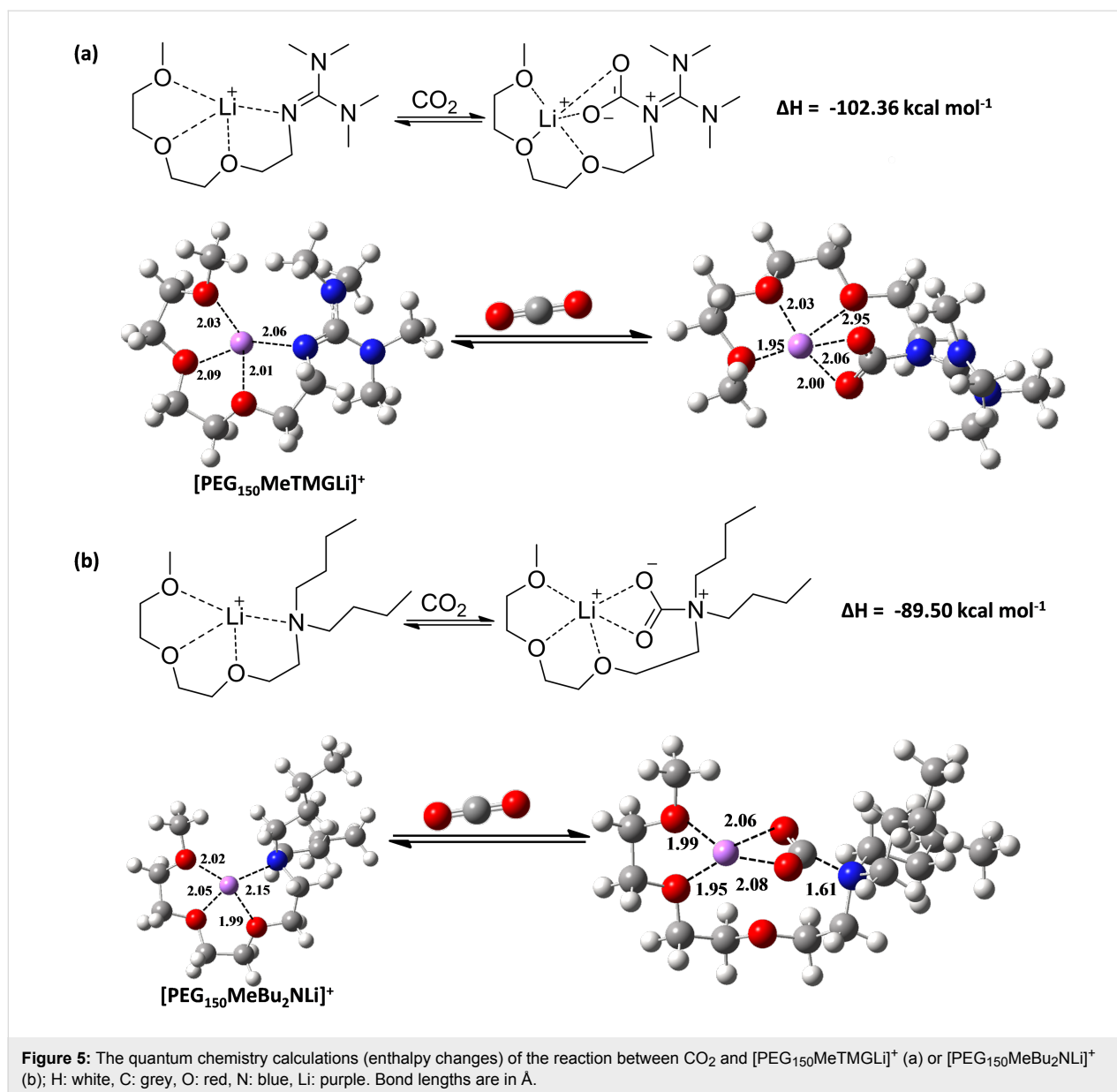
Experimental
Materials
All reagents used in this work were purchased from Sigma-Aldrich and used without further purification. CO$_2$ with a purity of 99.999% was obtained commercially.

Experimental methods
^{1}H NMR spectra were recorded on a Brucker 400 spectrometer in CDCl$_3$. Residual CHCl$_3$ (7.26 ppm) was used as internal reference. ^{13}C NMR spectra were recorded at 100.6 MHz in CDCl$_3$. Residual CHCl$_3$ (77.0 ppm) was used as internal reference. In situ FTIR spectra were collected on a Mettler Toledo React IR ic10, which was equipped with a diamond ATR probe, using an ic IR analysis system. The probe was placed into the absorption mixture. Spectra were collected in situ during CO$_2$ absorption, while the mixture was stirred continuously using a magnetic stir bar. ESI-MS spectra were recorded on a Thermo Finnigan LCQ Advantage spectrometer in ESI mode at a spray voltage of 4.8 kV.

General procedure for CO$_2$ absorption
The CO$_2$ absorption procedure was analogous to the CO$_2$/SO$_2$ absorption procedure we had reported before [35,44]. In a typical procedure, the CO$_2$ capture was carried out in a 10 mL Schlenk flask. The absorbents were charged into the reactor at room temperature. Then, the air in the flask was replaced by passing CO$_2$ through a needle, which was inserted into the bottom of the flask. The absorption was conducted at 25 °C with a CO$_2$ flow rate of 0.1 L/min. The amount of CO$_2$

Figure 5: The quantum chemistry calculations (enthalpy changes) of the reaction between CO_2 and $[PEG_{150}MeTMGLi]^+$ (a) or $[PEG_{150}MeBu_2NLi]^+$ (b); H: white, C: grey, O: red, N: blue, Li: purple. Bond lengths are in Å.

absorbed was determined by following the weight of the mixture with an Analytical Balance. Data points were taken with an accuracy of ±0.0001 g every five minutes. Absorption/desorption was determined for at least three cycles.

Supporting Information

Supporting Information File 1

General experimental methods, synthesis and characterization of the neutral ligands, lithium salts and the corresponding chelated ionic liquids.
[http://www.beilstein-journals.org/bjoc/content/supplementary/1860-5397-10-204-S1.pdf]

Acknowledgements

References

1. Raupach, M. R.; Marland, G.; Ciais, P.; Le Quéré, C.; Canadell, J. G.; Klepper, G.; Field, C. B. *Proc. Natl. Acad. Sci. U. S. A.* **2007,** *104,* 10288–10293. doi:10.1073/pnas.0700609104
2. Yang, Z.-Z.; Zhao, Y.-N.; He, L.-N. *RSC Adv.* **2011,** *1,* 545–567. doi:10.1039/c1ra00307k
3. Yang, Z.-Z.; He, L.-N.; Gao, J.; Liu, A.-H.; Yu, B. *Energy Environ. Sci.* **2012,** *5,* 6602–6639. doi:10.1039/C2EE02774G

4. D'Alessandro, D. M.; Smit, B.; Long, J. R. *Angew. Chem., Int. Ed.* **2010,** *49,* 6058–6082. doi:10.1002/anie.201000431

5. Choi, S.; Drese, J. H.; Jones, C. W. *ChemSusChem* **2009,** *2,* 796–854. doi:10.1002/cssc.200900036

6. Wang, Q.; Luo, J.; Zhong, Z.; Borgna, A. *Energy Environ. Sci.* **2011,** *4,* 42–55. doi:10.1039/c0ee00064g

7. Li, L.; Zhao, N.; Wei, W.; Sun, Y. *Fuel* **2013,** *108,* 112–130. doi:10.1016/j.fuel.2011.08.022

8. Welton, T. *Chem. Rev.* **1999,** *99,* 2071–2084. doi:10.1021/cr980032t

9. Wasserscheid, P.; Keim, W. *Angew. Chem., Int. Ed.* **2000,** *39,* 3772–3789. doi:10.1002/1521-3773(20001103)39:21<3772::AID-ANIE3772>3.0.CO;2-5

10. Petkovic, M.; Seddon, K. R.; Rebelo, L. P. N.; Pereira, C. S. *Chem. Soc. Rev.* **2011,** *40,* 1383–1403. doi:10.1039/c004968a

11. Plechkova, N. V.; Seddon, K. R. *Chem. Soc. Rev.* **2008,** *37,* 123–150. doi:10.1039/b006677j

12. Ma, Z.; Yu, J.; Dai, S. *Adv. Mater.* **2010,** *22,* 261–285. doi:10.1002/adma.200900603

13. Antonietti, M.; Kuang, D.; Smarsly, B.; Zhou, Y. *Angew. Chem., Int. Ed.* **2004,** *43,* 4988–4992. doi:10.1002/anie.200460091

14. Dupont, J.; de Souza, R. F.; Suarez, P. A. Z. *Chem. Rev.* **2002,** *102,* 3667–3692. doi:10.1021/cr010338r

15. Zakrzewska, M. E.; Bogel-Łukasik, E.; Bogel-Łukasik, R. *Chem. Rev.* **2011,** *111,* 397–417. doi:10.1021/cr100171a

16. Miao, C.-X.; He, L.-N.; Wang, J.-Q.; Wang, J.-L. *Adv. Synth. Catal.* **2009,** *351,* 2209–2216. doi:10.1002/adsc.200900285

17. Zhang, Q.; Zhang, S.; Deng, Y. *Green Chem.* **2011,** *13,* 2619–2637. doi:10.1039/c1gc15334j

18. Han, X.; Armstrong, D. W. *Acc. Chem. Res.* **2007,** *40,* 1079–1086. doi:10.1021/ar700044y

19. Berthod, A.; Ruiz-Ángel, M. J.; Carda-Broch, S. *J. Chromatogr., A* **2008,** *1184,* 6–18. doi:10.1016/j.chroma.2007.11.109

20. Armand, M.; Endres, F.; MacFarlane, D. R.; Ohno, H.; Scrosati, B. *Nat. Mater.* **2009,** *8,* 621–629. doi:10.1038/nmat2448

21. MacFarlane, D. R.; Forsyth, M.; Howlett, P. C.; Pringle, J. M.; Sun, J.; Annat, G.; Neil, W.; Izgorodina, E. I. *Acc. Chem. Res.* **2007,** *40,* 1165–1173. doi:10.1021/ar7000952

22. Ramdin, M.; de Loos, T. W.; Vlugt, T. J. H. *Ind. Eng. Chem. Res.* **2012,** *51,* 8149–8177. doi:10.1021/ie3003705

23. Bates, E. D.; Mayton, R. D.; Ntai, I.; Davis, J. H., Jr. *J. Am. Chem. Soc.* **2002,** *124,* 926–927. doi:10.1021/ja017593d

24. Zhang, X.; Zhang, X.; Dong, H.; Zhao, Z.; Zhang, S.; Huang, Y. *Energy Environ. Sci.* **2012,** *5,* 6668–6681. doi:10.1039/c2ee21152a

25. Zhang, J.; Zhang, S.; Dong, K.; Zhang, Y.; Shen, Y.; Lv, X. *Chem. – Eur. J.* **2006,** *12,* 4021–4026. doi:10.1002/chem.200501015

26. Jiang, Y.-Y.; Wang, G.-N.; Zhou, Z.; Wu, Y.-T.; Geng, J.; Zhang, Z.-B. *Chem. Commun.* **2008,** 505–507. doi:10.1039/b713648j

27. Zhang, Y.; Zhang, S.; Lu, X.; Zhou, Q.; Fan, W.; Zhang, X. *Chem. – Eur. J.* **2009,** *15,* 3003–3011. doi:10.1002/chem.200801184

28. Yu, H.; Wu, Y.-T.; Jiang, Y.-Y.; Zhou, Z.; Zhang, Z.-B. *New J. Chem.* **2009,** *33,* 2385–2390. doi:10.1039/b9nj00330d

29. Li, X.; Hou, M.; Zhang, Z.; Han, B.; Yang, G.; Wang, X.; Zou, L. *Green Chem.* **2008,** *10,* 879–884. doi:10.1039/b801948g

30. Luo, X. Y.; Ding, F.; Lin, W. J.; Qi, Y. Q.; Li, H. R.; Wang, C. M. *J. Phys. Chem. Lett.* **2014,** *5,* 381–386. doi:10.1021/jz402531n

31. Wang, C.; Mahurin, S. M.; Luo, H.; Baker, G. A.; Li, H.; Dai, S. *Green Chem.* **2010,** *12,* 870–874. doi:10.1039/b927514b

32. Wang, C.; Luo, H.; Luo, X.; Li, H.; Dai, S. *Green Chem.* **2010,** *12,* 2019–2023. doi:10.1039/c0gc00070a

33. Wang, C.; Luo, H.; Jiang, D.-e.; Li, H.; Dai, S. *Angew. Chem., Int. Ed.* **2010,** *49,* 5978–5981. doi:10.1002/anie.201002641

34. Wang, C.; Luo, X.; Luo, H.; Jiang, D.-e.; Li, H.; Dai, S. *Angew. Chem., Int. Ed.* **2011,** *50,* 4918–4922. doi:10.1002/anie.201008151

35. Yang, Z.-Z.; He, L.-N.; Zhao, Y.-N.; Li, B.; Yu, B. *Energy Environ. Sci.* **2011,** *4,* 3971–3975. doi:10.1039/C1EE02156G

36. Gurkan, B. E.; de la Fuente, J. C.; Mindrup, E. M.; Ficke, L. E.; Goodrich, B. F.; Price, E. A.; Schneider, W. F.; Brennecke, J. F. *J. Am. Chem. Soc.* **2010,** *132,* 2116–2117. doi:10.1021/ja909305t

37. Liu, A.-H.; Ma, R.; Song, C.; Yang, Z.-Z.; Yu, A.; Cai, Y.; He, L.-N.; Zhao, Y.-N.; Yu, B.; Song, Q.-W. *Angew. Chem., Int. Ed.* **2012,** *51,* 11306–11310. doi:10.1002/anie.201205362

38. Wang, C.; Guo, Y.; Zhu, X.; Cui, G.; Li, H.; Dai, S. *Chem. Commun.* **2012,** *48,* 6526–6528. doi:10.1039/c2cc32365f

39. Yang, Z.-Z.; Jiang, D.-e.; Zhu, X.; Tian, C.; Brown, S.; Do-Thanh, C.-L.; He, L.-N.; Dai, S. *Green Chem.* **2014,** *16,* 253–258. doi:10.1039/c3gc41513a

40. Das Neves Gomes, C.; Jacquet, O.; Villiers, C.; Thuéry, P.; Ephritikhine, M.; Cantat, T. *Angew. Chem., Int. Ed.* **2012,** *51,* 187–190. doi:10.1002/anie.201105516

41. Villiers, C.; Dognon, J.-P.; Pollet, R.; Thuéry, P.; Ephritikhine, M. *Angew. Chem., Int. Ed.* **2010,** *49,* 3465–3468. doi:10.1002/anie.201001035

42. Rainbolt, J. E.; Koech, P. K.; Yonker, C. R.; Zheng, F.; Main, D.; Weaver, M. L.; Linehan, J. C.; Heldebrant, D. J. *Energy Environ. Sci.* **2011,** *4,* 480–484. doi:10.1039/c0ee00506a

43. Blanchard, L. A.; Gu, Z.; Brennecke, J. F. *J. Phys. Chem. B* **2001,** *105,* 2437–2444. doi:10.1021/jp003309d

44. Yang, Z.-Z.; He, L.-N.; Zhao, Y.-N.; Yu, B. *Environ. Sci. Technol.* **2013,** *47,* 1598–1605. doi:10.1021/es304147q